

Efficient construction of Bayes optimal designs for stochastic process models

C. S. Gillespie* & R. J. Boys

School of Mathematics, Statistics & Physics, Newcastle University,
Newcastle upon Tyne, NE1 7RU, UK

Stochastic process models are now commonly used to analyse complex biological, ecological and industrial systems. Increasingly there is a need to deliver accurate estimates of model parameters and assess model fit by optimizing the timing of measurement of these processes. Standard methods to construct Bayes optimal designs, such the well known Müller algorithm, are computationally intensive even for relatively simple models. A key issue is that, in determining the merit of a design, the utility function typically requires summaries of many parameter posterior distributions, each determined via a computer-intensive scheme such as MCMC. This paper describes a fast and computationally efficient scheme to determine optimal designs for stochastic process models. The algorithm compares favourably with other methods for determining optimal designs and can require up to an order of magnitude fewer utility function evaluations for the same accuracy in the optimal design solution. It benefits from being embarrassingly parallel and is ideal for running on the cloud. The method is illustrated by determining different sized optimal designs for three problems of increasing complexity.

Keywords: observation times, particle representation, prior predictive distribution, utility function

1 Introduction

Stochastic process models are increasingly used to describe the dynamic evolution of a complex system containing different interacting species. Applications appear in many areas such as biology, ecology, pharmacokinetics and industry; see, for example, Henderson et al. (2009), Cook et al. (2008), Ryan et al. (2015) and Khatab et al. (2017). Designed experiments can be very useful to the practitioner as they allow them to learn about models and their parameters in an efficient way. For example, in systems biology, an experimenter might build a stochastic kinetic model for their biological system; these models are typically described through a series of reactions between the species, with each reaction depending on an unknown stochastic rate constant. Data are then collected with the aim of estimating these constants and assessing model fit. Clearly scheduling the timing of say k observations within a $(0, T)$ experimental time period has the potential to yield much more accurate inferences than say just observing the process at k times on a regular grid.

We consider designs in which the stochastic process is observed on k occasions, at times $\mathbf{d} = (t_1, \dots, t_k)$. In general, the merit of a particular design \mathbf{d} is captured through a utility function

*email: colin.gillespie@newcastle.ac.uk

Algorithm 1 MCMC algorithm by Müller (1999)

- 1: Initialise \mathbf{d}^0 , simulate $\mathbf{y}_1^0, \dots, \mathbf{y}_J^0 \overset{\text{indep}}{\sim} \pi(\mathbf{y}|\mathbf{d}^0)$
 - 2: Calculate $u^0 = \prod_{j=1}^J u(\mathbf{d}^0, \mathbf{y}_j^0)$
 - 3: **for** $i = 1$ to N **do**
 - 4: Propose $\mathbf{d}^* \sim q(\mathbf{d}|\mathbf{d}^{i-1})$ and simulate $\mathbf{y}_1^*, \dots, \mathbf{y}_J^* \overset{\text{indep}}{\sim} \pi(\mathbf{y}|\mathbf{d}^*)$
 - 5: Calculate $u^* = \prod_{j=1}^J u(\mathbf{d}^*, \mathbf{y}_j^*)$
 - 6: **if** $U(0, 1) < \min(1, u^*q(\mathbf{d}^{i-1}|\mathbf{d}^*)/\{u^{i-1}q(\mathbf{d}^*|\mathbf{d}^{i-1})\})$
 - 7: **then** $u^i = u^*$, $\mathbf{d}^i = \mathbf{d}^*$ **else** $u^i = u^{i-1}$, $\mathbf{d}^i = \mathbf{d}^{i-1}$
 - 8: **end**
-

$u(\mathbf{d}, \mathbf{y}, \boldsymbol{\theta})$, where \mathbf{y} are data that might be observed at times \mathbf{d} when the model parameter is $\boldsymbol{\theta}$. In this paper we focus on a utility function based on the posterior distribution of $\boldsymbol{\theta}$, namely, the posterior generalised precision $u(\mathbf{d}, \mathbf{y}) = 1/\det\{\text{Var}(\boldsymbol{\theta}|\mathbf{y}, \mathbf{d})\}$. This utility has an intuitive motivation and is appropriate if the posterior is unimodal and without substantial skewness or kurtosis. Note that this utility function does not depend on the model parameter $\boldsymbol{\theta}$.

As the choice of design must be made before observing data, designs should be assessed by their expected utility

$$u(\mathbf{d}) = E_{\mathbf{y}}\{u(\mathbf{d}, \mathbf{y})\} = \int_{\mathbf{y}} u(\mathbf{d}, \mathbf{y})\pi(\mathbf{y}|\mathbf{d}) d\mathbf{y},$$

where $\pi(\mathbf{y}|\mathbf{d}) = \int_{\boldsymbol{\theta}} \pi(\mathbf{y}|\mathbf{d}, \boldsymbol{\theta})\pi(\boldsymbol{\theta})d\boldsymbol{\theta}$ is the prior predictive density of the unobserved data, $\pi(\mathbf{y}|\mathbf{d}, \boldsymbol{\theta})$ is the density of the unobserved data \mathbf{y} when using design \mathbf{d} and the model parameter is $\boldsymbol{\theta}$, and $\pi(\boldsymbol{\theta})$ is the prior density describing uncertainty in the model parameter. Therefore the optimal design \mathbf{d}^* over a design space \mathcal{D} is given by

$$\mathbf{d}^* = \arg \max_{\mathbf{d} \in \mathcal{D}} u(\mathbf{d}).$$

Unfortunately the expected utility $u(\mathbf{d})$ is rarely analytically tractable and so computational schemes are needed. As standard Monte Carlo integration methods are also not feasible for non-trivial problems, Müller (1999) proposed a Monte Carlo Markov chain (MCMC) approach. Although the general Müller scheme allows for the utility function to depend on $\boldsymbol{\theta}$, here we focus on utility functions which depend only on the design \mathbf{d} and potential observations \mathbf{y} . In this scenario the Müller scheme targets the density

$$h(\mathbf{d}, \mathbf{y}) \propto u(\mathbf{d}, \mathbf{y})\pi(\mathbf{y}|\mathbf{d})$$

using the MCMC scheme in Algorithm 1 (with $J = 1$). The key feature of this scheme is that the marginal distribution over \mathbf{y} is proportional to the expected utility $u(\mathbf{d})$. Therefore the optimal design can be estimated as the mode of the empirical marginal for \mathbf{d} , obtained from the MCMC sample. Note that this scheme mixes over design space by proposing moves using a proposal distribution q for designs. Also realisations from the prior predictive distribution of the unobserved data $\pi(\mathbf{y}|\mathbf{d})$ are obtained straightforwardly by first simulating a parameter value $\boldsymbol{\theta}$ from the prior distribution and then data \mathbf{y} from the stochastic model. Müller suggested that this mode might be identified more easily by using $J > 1$ replicates from the prior predictive distribution. Here the MCMC scheme target becomes

$$h_J(\mathbf{d}, \mathbf{y}_1, \dots, \mathbf{y}_J) \propto \prod_{j=1}^J u(\mathbf{d}, \mathbf{y}_j)\pi(\mathbf{y}_j|\mathbf{d}).$$

Algorithm 2 Step m of the Resampling-Markov algorithm by Amzal et al. (2006)

```
1: for  $i = 1$  to  $N$  do
2:   Simulate  $\mathbf{y}_{ij}^{m-1} \stackrel{\text{indep}}{\sim} \pi(\mathbf{y}|\mathbf{d}_i^{m-1})$ ,  $j = J_{m-1} + 1, \dots, J_m$ 
3:   Calculate  $w_i^m = w_i^{m-1} \prod_{j=J_{m-1}+1}^{J_m} u(\mathbf{d}_i^{m-1}, \mathbf{y}_{ij}^{m-1})$ 
4: end
5: Simulate  $(\ell_1, \dots, \ell_N) \sim M(N, \mathbf{w}^m)$ 
6: for  $i = 1$  to  $N$  Set  $\widehat{\mathbf{d}}_i = \mathbf{d}_{\ell_i}$  and  $\widehat{w}_i^m = \widehat{w}_{\ell_i}^{m-1} \times w_{\ell_i}^m$ 
7: for  $i = 1$  to  $N$  do
8:   Simulate  $\overline{\mathbf{d}}_i^m \sim q_{MH}(\mathbf{d}|\widehat{\mathbf{d}}_i^m)$  and  $\overline{\mathbf{y}}_{ij}^m \stackrel{\text{indep}}{\sim} \pi(\mathbf{y}|\overline{\mathbf{d}}_i^m)$ ,  $j = 1, \dots, J_m$ 
9:   Calculate  $\overline{w}_i^m = \prod_{j=1}^{J_m} u(\overline{\mathbf{d}}_i^m, \overline{\mathbf{y}}_{ij}^m)$ 
10:  Calculate  $\alpha_i = \min[1, \{\overline{w}_i^m q_{MH}(\widehat{\mathbf{d}}_i^m | \overline{\mathbf{d}}_i^m)\} / \{\widehat{w}_i^m q_{MH}(\overline{\mathbf{d}}_i^m | \widehat{\mathbf{d}}_i^m)\}]$ 
11:  if  $U(0, 1) < \alpha_i$  then  $\mathbf{d}_i^m = \overline{\mathbf{d}}_i^m$  else  $\mathbf{d}_i^m = \widehat{\mathbf{d}}_i^m$ 
12: end
```

The marginal for \mathbf{d} is now proportional to $u(\mathbf{d})^J$ and so, as J increases, the variance of this marginal is reduced and the mode is identified more easily. However, a significant problem with this algorithm is that, for large J , the computational burden becomes prohibitive and the algorithm risks getting stuck in a local mode.

More recently, Amzal et al. (2006) developed a particle-based approach to target $h_J(\mathbf{d})$. Their method begins by first setting a list of increasing values of J : $J_1 < J_2 < \dots < J_M$. The main loop in their Resampling-Markov algorithm starts with a sample drawn approximately from $h_{J_{m-1}}(\mathbf{d})$ that is then resampled and enriched by a Markov step (with proposal distribution q_{MH}) to become an approximated sample from $h_{J_m}(\mathbf{d})$. The algorithm for a particular choice of J is given in Algorithm 2. This algorithm has many strengths over the standard Müller algorithm, particularly in that it adaptively searches for the optimal design.

2 Efficiency improvements to the algorithm

We now describe a new algorithm which also uses a particle-based approach but is one that is much more straightforward, makes more efficient use of evaluations of the utility function and also more efficiently identifies near-optimal designs. Essentially the approach bases particle weights on current estimates of expected utility and thereby focuses sampling effort around near-optimal designs.

Consider the general case where we need an optimal k -timepoint design $\mathbf{d} = (t_1, \dots, t_k)$, where the times t_i must lie on a grid rather than in a continuous interval. This restriction reflects the practical nature of experimentation but, of course, near continuous designs may be found by using a grid with a fine mesh. The algorithm uses refinements of a particle distribution to increasingly focus on designs around the optimal design. Instead of basing the weights on increasing powers of the utility function, we focus on designs with (current estimated) expected utility values in the upper $100\alpha_m\%$ of their distribution. The algorithm targets near optimal designs by working through a series of steps in which the α_m -values decrease as the step number m increases; for example, we take $\alpha_m = 2^{-m}$. The powering-up technique used by Müller (1999) and Amzal et al. (2006) is their way of focusing on designs which are near optimal. Although we could use a similar technique which calculates weights by powering-up current estimates of the expected utility, we feel that it is more natural and intuitive to deal directly with the size of the upper tail of the distribution of the expected utility.

Suppose the location of a design on the discretised mesh of timepoints is defined by the coordinate

Algorithm 3 Step m of new algorithm

```
1:  $\mathbf{w}^m = \mathbf{w}^{m-1}$ 
2: for  $i = 1$  to  $N_m$  do (in parallel)
3:   Simulate  $\ell^* \sim \text{Cat}(\mathbf{w}^m)$ 
4:   Simulate  $\ell \sim q(\ell|\ell^*)$  and  $\mathbf{y} \sim \pi(\mathbf{y}|\mathbf{d}_\ell)$ 
5:   Calculate  $u(\mathbf{d}_\ell, \mathbf{y})$ 
6:   Update expected utility  $\hat{u}(\mathbf{d}_\ell) \leftarrow \{u(\mathbf{d}_\ell, \mathbf{y}) + n_\ell \hat{u}(\mathbf{d}_\ell)\} / \{n_\ell + 1\}$ 
7:   Update count  $n_\ell \leftarrow n_\ell + 1$ 
8:   Update weights  $\mathbf{w}^m$  to contain top  $100\alpha_m\%$  values of  $\{\hat{u}(\mathbf{d}_k) : n_k > 0\}$ 
9: end
```

system $\ell = (\ell_1, \dots, \ell_k)$ for $\ell \in \mathbf{L}$ so that the design space is $\mathcal{D} = \{\mathbf{d}_\ell : \ell \in \mathbf{L}\}$. The algorithm works with a (discrete) k -dimensional categorical distribution in which the design at location ℓ has probability $p(\ell) = w_\ell$. This distribution is initialised to be a discrete uniform $\text{Cat}_k(\mathbf{w}^0)$ distribution, with un-normalised weights $w_\ell^0 = 1$, and mass function $p(\ell) \propto w_\ell^0$, $\ell \in \mathbf{L}$. Note that this choice is an exchangeable one and reflects the inability to choose between designs initially.

The algorithm begins with $m = 1$ and first chooses the location of designs (at which utility calculations are to be made) by taking a random sample from the $\text{Cat}_k(\mathbf{w}^0)$ distribution. After simulating datasets from the prior predictive distribution at these designs, the results of the utility calculations (at these designs) are then used to initialise the estimate of the expected utility $\hat{u}(\mathbf{d}_\ell) = \text{mean}(u_{\ell_k} : \ell_k = \ell)$. Note that any designs not visited during this step of the algorithm are given a zero expected utility. The current values of the (estimated) expected utilities are then used to construct the particle distribution at the next step, $\text{Cat}_k(\mathbf{w}^1)$, by taking $w_\ell^1 = \hat{u}(\mathbf{d}_\ell)$ for those designs \mathbf{d}_ℓ with (estimated) expected utilities in the top $100\alpha_1\%$ of their distribution and $w_\ell^1 = 0$ for all other designs. Note that the accuracy of the estimates of expected utility will depend on the number of times the design at this location is visited during the algorithm. The above description is step $m = 1$ in a general algorithm which, at step $m = 1, \dots, M$, runs the algorithm (with $\alpha = \alpha_m$) by first choosing designs at locations according to a $\text{Cat}_k(\mathbf{w}^{m-1})$ distribution. Of course, given the size of the design space, it is possible that many near optimal designs are not chosen and so giving these designs zero weight is not sensible. We therefore perturb the sampled locations by using a distribution q which, for example, might move a design to one of its 2^k neighbouring locations, and thereby reach local near-optimal designs. More generally we can use a random walk proposal such as $q(\mathbf{d}_{\ell^*}|\mathbf{d}_\ell) = \prod_{i=1}^k q_i(\ell_i^*|\ell_i)$ over design locations, where each $q_i(\ell_i^*|\ell_i)$ is a symmetric univariate random walk proposal, to tailor the size of the local search and help to reach and stay fairly close to near-optimal designs. Utilities are then calculated by first simulating datasets from the prior predictive distribution at these design locations and these utilities used to construct the $\text{Cat}(\mathbf{w}^m)$ distribution at the next step, where $w_\ell^m = w_\ell^{m-1}$ for those designs \mathbf{d}_ℓ with (estimated) expected utilities in the top $100\alpha_m\%$ of their distribution and $w_\ell^m = 0$ for all other designs. Finally, after completing all M steps, we take the optimal design as $\mathbf{d}^* = \mathbf{d}_{\ell^*}$, where $\ell^* = \arg \max_\ell w_\ell^M$, or conduct a final more intensive search around this putative optimal design.

The Müller and Resampling-Markov algorithms do not make use of utility calculations made at design locations in previous steps. Thus a simple but productive efficiency improvement can be made by using all utility calculations made in previous steps of the algorithm. This is easily done by keeping a running average of the utility calculations at each design location. Additional improvements can be made by using all computer cores available to the user. For example, if C cores are available, there is little additional time penalty in calculating C utilities $u(\mathbf{d}_{\ell_k}, \mathbf{y}_k)$ rather than just one. Finally, another efficiency gain may be achieved by using a different run length N_m in each step, with the earlier steps perhaps using longer runs. However, the rate at which the N_m

decrease should depend on the extent to which reducing α_m identifies a clear optimal design. A summary of the new algorithm is given in Algorithm 3. Although we could leave updating the weights until the next step of the algorithm, we have found it beneficial to update the current weights \mathbf{w}^m regularly, leading to line 8 being within the main loop.

In general, the initial uniform $Cat_k(\mathbf{w}^0)$ distribution over design locations will work reasonably well so long as the number of possible designs $|\mathcal{D}|$ is not too large. However, if $|\mathcal{D}|$ is large, for example when using a reasonably fine time-grid and seeking a design with a moderate number of timepoints, making sure that the algorithm visits all near-optimal designs in step 1 could become problematic. That said, we have found that expanding the reach of the local random walk proposals deals with this issue quite well, though this inevitably leads to needing a larger number of iterations N_m .

3 Examples

We demonstrate the efficiency of our method by determining optimal designs of different sizes in three model scenarios. We begin by studying the death model considered by Cook et al. (2008) and Drovandi and Pettitt (2013). This simple model has a tractable likelihood and so calculation of the posterior variance, and hence the utility function, is straightforward. We consider in detail the case of determining an optimal single timepoint and compare the accuracy of our new method with those of other popular methods. We then consider optimal design for a more complex stochastic model of aphid growth (Matis et al., 2007). Here we calculate the posterior variance using a moment closure approximation to the stochastic model and determine optimal designs of different sizes using multi-core parallel computing, enabling a six-fold speed-up. Finally we consider a pharmacokinetic model of extra-corporeal membrane oxygenation in sheep (Ryan et al., 2015). Here the posterior variance is estimated from the output of an MCMC scheme. We determine a $k = 10$ timepoint design but, due to its size, constrain the timepoints to be percentiles of a Beta(a, b) distribution scaled to cover the full observation period $(0, T)$. Thus the optimal design here is determined by appropriate choice of the parameters a and b . In this case the utility function is more time-consuming to estimate and so we move the computations to the cloud. This enables us to simultaneously use over 150 CPU cores, giving a proportionate speed-up.

3.1 Death model

Cook et al. (2008) describe a death model in which the size $Y(t)$ of the population at time t obeys the probabilistic law: in the small time period $(t, t + \delta t]$, the probability of a death is $Pr\{Y(t + \delta t) = i - 1 | Y(t) = y(t)\} = \beta y(t) \delta t + o(\delta t)$, otherwise no death occurs. If the population is initialised with size $n = Y(t_0 = 0)$ and then observed at times t_1, \dots, t_k , the likelihood is formed from terms $Y(t_k) | Y(t_{k-1}) = y_{k-1} \sim Bin\{y_{k-1}, \exp[-\beta(t_k - t_{k-1})]\}$.

Suppose interest lies in determining the optimal k -timepoint design $\mathbf{d} = (t_1, \dots, t_k)$ using the posterior precision of β as our utility function, that is, $u(\mathbf{d}, \mathbf{y}) = 1/\text{Var}(\beta | \mathbf{y})$. One considerable benefit of studying this model is that values of the expected utility can be calculated and there is no need to employ a stochastic algorithm such as an MCMC algorithm or importance sampling. It is fairly quick to calculate $K_i(\mathbf{y}) = \int \beta^i \pi(\mathbf{y} | \beta) \pi(\beta) d\beta$, $i = 0, 1, 2$ over all possible $\mathbf{y} = (y_{t_1}, \dots, y_{t_k})$ using the GSL library (Galassi et al., 1996). Thus we can calculate the expected utility over all possible designs \mathbf{d} using

$$u(\mathbf{d}) = \sum_{y_{t_1} \geq \dots \geq y_{t_k} = 0}^n \pi(\mathbf{y}) u(\mathbf{d}, \mathbf{y}) = \sum_{y_{t_1} \geq \dots \geq y_{t_k} = 0}^n \frac{K_0(\mathbf{y})^3}{K_2(\mathbf{y})K_0(\mathbf{y}) - K_1(\mathbf{y})^2}, \quad (1)$$

where n is the initial population size, and thereby determine the optimal k -timepoint design \mathbf{d}^* .

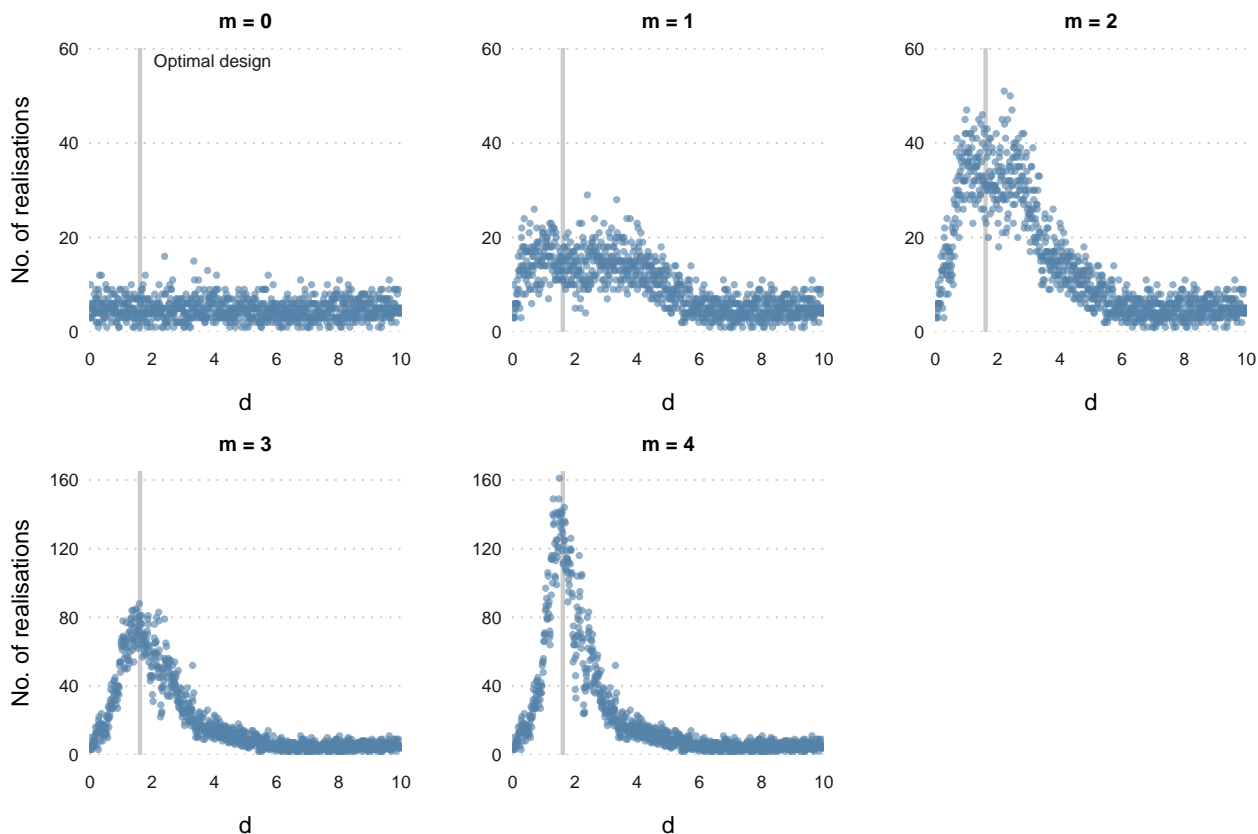


Figure 1: Graphs showing the number of realisations $u(d, y_i)$ contributing to the estimate of $u(d)$ at each d as the number of steps m increases. The vertical grey line shows the optimal design ($d^* = 1.61$).

We follow Drovandi and Pettitt (2013) by considering an experimental period over $(0, T = 10)$ and restrict design timepoints to be on the grid $t = 0.01(0.01)10$. The initial population size is fixed to be $n = 50$. We also take their log-normal $\text{LN}(-0.005, 0.01)$ prior distribution for β and focus on determining the optimal single ($k = 1$) timepoint design. This problem is sufficiently simple that it is possible to calculate the expected utility for each possible single timepoint design and determine that the optimal single timepoint design is $d^* = t_1^* = 1.61$.

Figure 1 shows how the new algorithm increasingly focuses on getting ever more accurate estimates of near optimal expected utilities (by averaging over more realisations from the prior predictive distribution) over steps $m = 0, 1, 2, 3, 4$ of the algorithm, with $\alpha_m = 2^{-m}$. The plot for the initial $m = 0$ step shows the (near) uniform coverage over all possible timepoints and then, as m increases, more and more realisations are simulated at near-optimal timepoints. After the $m = 4$ step, the estimate of expected utility at $t_1^* = 1.61$ is an average over 160 realisations of $u(t_1^* = 1.61, y)$.

Figure 2 gives a comparison of the performance of the Müller, Amzal and our new algorithms by showing the sampling distribution of the optimal designs they return over 500 independent runs of each algorithm. Each run of each algorithm uses the same computational budget of 24K utility evaluations and takes approximately the same run time. For comparison purposes we also give results for the approximate coordinate exchange (ACE) algorithm (Overstall and Woods, 2017) implemented using the R package `acebayes` (Overstall et al., 2017) with parameters $B = (200, 19)$ and $N_2 = 0$. The results from each algorithm use only a single CPU core. However, as mentioned previously, if more cores are available then our new algorithm scales trivially with the number of cores.

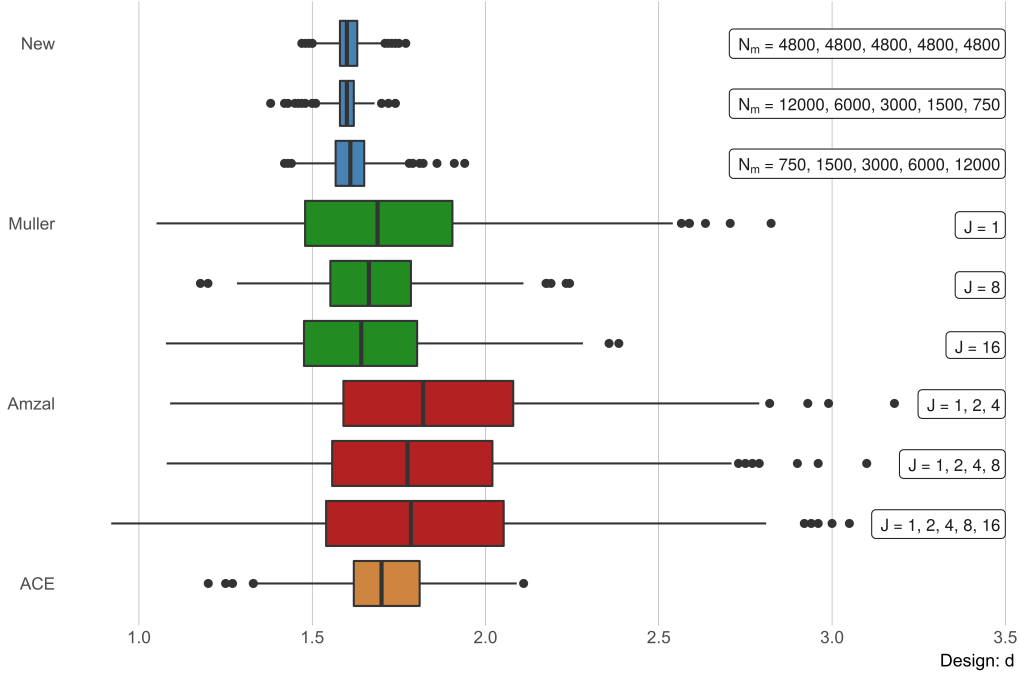


Figure 2: Box plots of the optimal designs returned by each algorithm from 500 independent runs. The correct optimal design is $d^* = 1.61$. The different cases are (a) New algorithm with $\alpha_m = 2^{-m}$ for (i) $N_m = 4800, 4800, 4800, 4800, 4800$; (ii) $N_m = 12000, 6000, 3000, 1500, 750$; (iii) $N_m = 750, 1500, 3000, 6000, 12000$. (b) Müller algorithm for $J = 1, 8, 16$. (c) Amzal algorithm for (i) $N_m = 2400, J_m = 1, 2, 4$; (ii) $N_m = 1090, J_m = 1, 2, 4, 8$; (iii) $N_m = 522, J_m = 1, 2, 4, 8, 16$. (d) Approximate coordinate exchange (ACE) algorithm with $B = (200, 19)$ and $N_2 = 0$.

The top three boxplots in Figure 2 summarise the results for the new algorithm but with different a breakdown of the 24K utility evaluations in each step $m = 0, 1, 2, 3, 4$. Overall the results show that the algorithm is fairly insensitive to the number (N_m) of evaluations in each step, though having the N_m decreasing in m appears to work best. Also the boxplots are tightly centered around the optimal design ($t_1^* = 1.61$). The next three boxplots are for the Müller algorithm with $J = 1, 8, 16$. It is clear that the spread of the Müller solutions is much larger than for the new algorithm. Another issue is that choosing an appropriate value for J would require tuning and therefore additional utility evaluations. The next three boxplots are for the Amzal algorithm using different powering up schemes with different numbers of steps (but still a total of 24K utility evaluations). Given the sophistication of the Amzal scheme it is surprising to see that its performance is similar to the Müller algorithm with $J = 1$. Inspection of the Amzal algorithm reveals that this is mainly due to the number of utility evaluations needed within the main loop (Algorithm 2, line 9). The bottom boxplot shows the results from the ACE algorithm using parameters given to us by the authors of the method. The variation in solutions from this algorithm is smaller than that of both Müller and Amzal. Perhaps a better overall objective measure of algorithm performance is their square root mean squared error (RMSE) about the correct solution $t_1^* = 1.61$. The values for these various implementations (in the order top-bottom in Figure 2) is New: 0.04, 0.07, 0.04, Müller: 0.33, 0.18, 0.24, Amzal: 0.43, 0.41, 0.44, ACE: 0.17 and show that the new algorithm can perform between 2.5

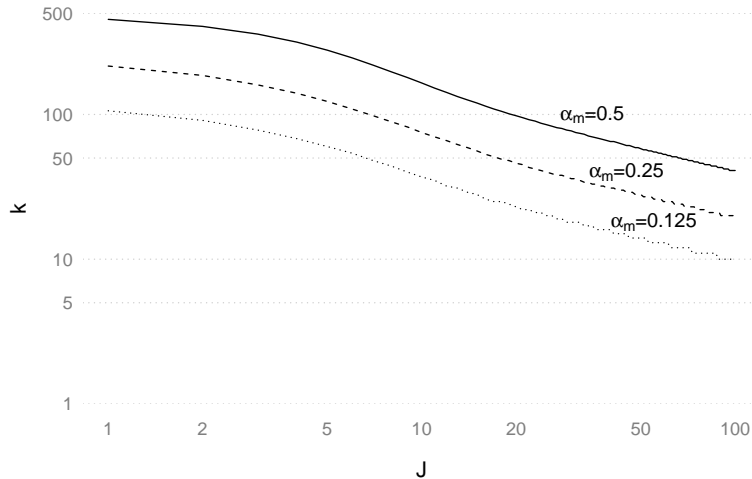


Figure 3: Relationship between the level of powering up (J) of the utility function in the Müller algorithm and, for the new algorithm, the number of designs (k) in the upper tail of the expected utility distribution, calculated over all 1000 single timepoint designs for the death model.

and 11 times more efficiently. An additional and powerful attribute of the new algorithm is that it is a much more simple algorithm to implement than the others and is embarrassingly parallel.

There is an indirect relationship between decreasing α_m in the new algorithm and Müller’s powering-up approach. Consider the normalised utility values $w_i^J = u(d_i) / \sum_{i'=1}^{|\mathcal{D}|} u^J(d_{i'})$, with order statistics $w_{(1)}^J \leq \dots \leq w_{(|\mathcal{D}|)}^J$ and empirical distribution function $\hat{F}_J(\cdot)$. A measure of the correspondence between the new algorithm and its Müller equivalent is the value of k , where

$$\arg \min_k \hat{F}_J \left\{ w_{(k)}^J \right\} > 1 - \alpha_m, \quad (2)$$

and α_m is the threshold used in step m of the new algorithm. The distribution of expected utility becomes increasingly peaked as $J \rightarrow \infty$, in which case $w_{(|\mathcal{D}|)}^J \rightarrow 1$, that is, $k \rightarrow |\mathcal{D}|$. Also during the $m = 1$ step of the new algorithm, designs are sampled from a distribution with weights proportional to (an estimate of) $u(d)$ and so this corresponds to the Müller algorithm with $J = 1$. In the Müller algorithm, as the expected utility is powered-up (by increasing J) the algorithm preferentially sample designs near the optimal design, that is, in the upper tail of the expected utility distribution. Unfortunately it is difficult to obtain an algebraic understanding of how increasing J focuses on designs further into the upper tail of the distribution of expected utility values, that is, its effect on k . However we can calculate the (exact) expected utility (for this simple death model) at all 1000 single timepoint designs in the design space using (1) and thereby determine values of k for different choices of J for various values of α_m ; see Figure 3. For example, when $\alpha_m = 0.5$ and $J = 1$, we obtain $k = 454$ as the sum of the largest 454 normalised utility values is greater than 0.5 (but that of the largest 453 is not). We see that k decreases as J increases (for fixed α_m). However for $J > 20$ the change in k drastically slows down. Furthermore, using values of $J > 100$, results in numerical issues. Also, although the traces in k for different α_m look parallel, they are only roughly parallel with, for example, $k_{\alpha=0.5} / k_{\alpha=0.25}$ ranging between 2.0 and 2.3. The figure highlights the main issue with the powering up approach: whilst being an intuitively good idea, in practice the rate at which this homes in on the optimal design as J increases is unclear and difficult to predict. Also working with large powers of utilities often introduces problems of numerical instability.

3.2 Cotton aphids

A cotton aphid infestation of a cotton plant can result in many problems such as leaves that curl and pucker, seedling plants become stunted and may die, a late season infestation can result in stained cotton. Also cotton aphids have developed resistance to many chemical treatments and so can be difficult to treat. Therefore considerable effort and cost is used in the maintenance of cotton plants. Matis et al. (2007) have developed a stochastic model of aphid population growth. Gillespie and Golightly (2010) give a Bayesian analysis of this model using data given in Matis et al. (2008). The data contain aphid counts on twenty randomly chosen leaves in each plot, for twenty-seven treatment-block combinations. The treatment-blocks were formed from three three-level factors (nitrogen and irrigation levels and block). Observations were taken roughly every 7 to 8 days within a 32 day period.

Let $N(t)$ and $C(t)$ denote the size and cumulative size of the aphid population respectively at time t . Matis et al. (2007) modelled aphid dynamics using a birth rate of $\lambda N(t)$ and a death rate of $\mu N(t)C(t)$. Therefore, in a small time period $(t, t + \delta t]$, so that at most one event can occur, we have

$$\begin{aligned} Pr\{N(t + \delta t) = n(t) + 1, C(t + \delta t) = c(t) + 1 | n(t), c(t)\} &= \lambda n(t) \delta t + o(\delta t), \\ Pr\{N(t + \delta t) = n(t) - 1, C(t + \delta t) = c(t) | n(t), c(t)\} &= \mu n(t) c(t) \delta t + o(\delta t), \end{aligned}$$

and the probability of staying in the same state is one minus the sum of these probabilities.

Gillespie and Golightly (2010) analysed these data by making a normal approximation to the stochastic model using moment closure. This gives transition distributions

$$(N(t_i), C(t_i))^T | N(t_{i-1}), C(t_{i-1}), \lambda, \mu \sim N_2\{\mathbf{m}(t_{i-1}), \mathbf{v}(t_{i-1})\},$$

where $\mathbf{m}(t) = (m_1(t) = E\{N(t)\}, m_2(t) = E\{C(t)\})^T$ and $\mathbf{v}(t)$ is a matrix with diagonal elements $v_{11}(t) = \text{Var}\{N(t)\}$ and $v_{22}(t) = \text{Var}\{C(t)\}$, and off-diagonal elements $v_{12}(t) = \text{Cov}\{N(t), C(t)\}$. Note that the (λ, μ) -dependence of these functions has been suppressed to simplify the exposition. These functions are determined as solutions of the ODE system

$$\begin{aligned} \frac{dm_1(t)}{dt} &= \lambda m_1(t) - \mu\{m_1(t)m_2(t) + v_{12}(t)\} \\ \frac{dm_2(t)}{dt} &= \lambda m_1(t) \\ \frac{dv_{11}(t)}{dt} &= \mu[v_{12}(t) - 2m_1(t)v_{12}(t) - 2\kappa_{21} + m_2(t)\{m_1(t) - 2v_{11}(t)\}] + \lambda\{m_1(t) + 2v_{11}(t)\} \\ \frac{dv_{12}(t)}{dt} &= \lambda\{m_1(t) + v_{11}(t) + v_{12}(t)\} - \mu\{m_1(t)v_{22}(t) + m_2(t)v_{12}(t)\} \\ \frac{dv_{22}(t)}{dt} &= \lambda\{m_1(t) + 2v_{12}(t)\}, \end{aligned} \tag{3}$$

with initial conditions $m_1(0) = n_0$, $m_2(0) = c_0$ and $v_{11}(0) = v_{12}(0) = v_{22}(0) = 0$. This system can be solved numerically using standard ODE solvers. Note that this approximation is the same as that when using the linear noise approximation if the term $v_{12}(t)$ in (3) is ignored.

We now construct optimal designs assuming a similar treatment-block pattern and observation period. The aim is to optimise the posterior generalised precision for the rate parameters $\boldsymbol{\theta} = (\lambda, \mu)$. Gillespie and Golightly (2010) found only small differences in the rate parameters for the various treatments and blocks and so we base our prior distribution on that of the posterior distribution for the base treatment and block rates, however we inflate prior uncertainty by increasing the variances by a factor of ten, giving

$$\begin{pmatrix} \lambda \\ \mu \end{pmatrix} \sim N_2 \left\{ \begin{pmatrix} 0.246 \\ 0.000134 \end{pmatrix}, \begin{pmatrix} 0.0079^2 & 5.8 \times 10^{-8} \\ 5.8 \times 10^{-8} & 0.00002^2 \end{pmatrix} \right\}.$$

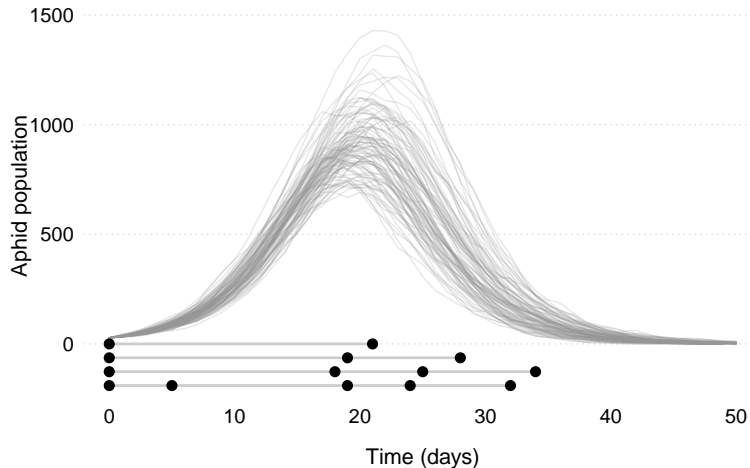


Figure 4: 100 prior predictive simulations together with the optimal one, two, three and four timepoint designs.

Also to simplify the analysis, we assume known initial aphid levels ($n_0 = c_0 = 28$) as there was very little variability in these quantities in the Matis et al. (2008) dataset.

One hundred simulations from the prior predictive are shown in Figure 4. All simulations ultimately end in the extinction of the aphid population, since the cumulative aphid population is increasing with each birth, resulting in $\mu n(t)c(t) > \lambda n(t)$ as t increases. All simulations show a peak in aphid population around 20–25 days.

The posterior density for the rate parameters when using a design with k timepoints yielding data \mathbf{y} is

$$\pi(\lambda, \mu | \mathbf{y}) \propto \pi(\lambda, \mu) \prod_{i=1}^k \phi_2\{n(t_i), c(t_i) | \mathbf{m}(t_{i-1}), \mathbf{v}(t_{i-1})\},$$

where $\phi_2(\cdot, \cdot | \mathbf{m}, \mathbf{v})$ is the $N_2(\mathbf{m}, \mathbf{v})$ density. Realisations from this posterior were obtained using an MCMC scheme with a bivariate normal random walk proposal, centred at the current value and a covariance matrix with standard deviations 0.0009 and 0.000004, and correlation equal to the prior correlation. We seek an optimal $k = 1, 2, 3, 4$ timepoint design within a $T = 49$ day period. Note that this period is slightly longer than that used in the original experiment to investigate whether the experiment was stopped too early. Thus the design timepoints are in units of 24 hours (called days) after the start of the new experiment (day zero). Again each posterior distribution was determined by initialising the chain at the parameter values used to simulate the responses \mathbf{y} and we found that very little burn-in was necessary. Each time the algorithm was run for 10K iterations, and typically took no more than 2 cpu seconds on a Intel Core i7-6700 CPU.

Again we determine the the optimal design using the predictive precision utility function $u(\mathbf{d}, \mathbf{y}) = 1/\det\{Var(\boldsymbol{\theta} | \mathbf{y})\}$. We look for one, two, three and four–timepoint optimal designs by moving through steps $m = 0, 1, \dots, 8$. In each step we use $N_m = 48\text{K}$ particles and therefore, in total, $9 \times 48\text{K} = 432\text{K}$ utility evaluations. The algorithm was run on a local high performance computer, using 20 Intel Xeon CPU E5-2690 cores.

Figure 5 shows the top 100 designs (or the top 50 designs in the case of the single time point design) with (rough) 95% confidence bounds (calculated assuming asymptotic posterior normality). Note that one of the benefits of using our algorithm is that it is straightforward to keep track of the precision of the current expected utility estimates by also keeping a running total of the $u(\mathbf{d}, \mathbf{y}_i)^2$. The figure shows that the confidence bounds for the one and two time point designs are very small. The intervals for the three point design are also relatively narrow. However, the optimal design is not clear and further runs will be needed to reduce uncertainty on the expected utility estimates.

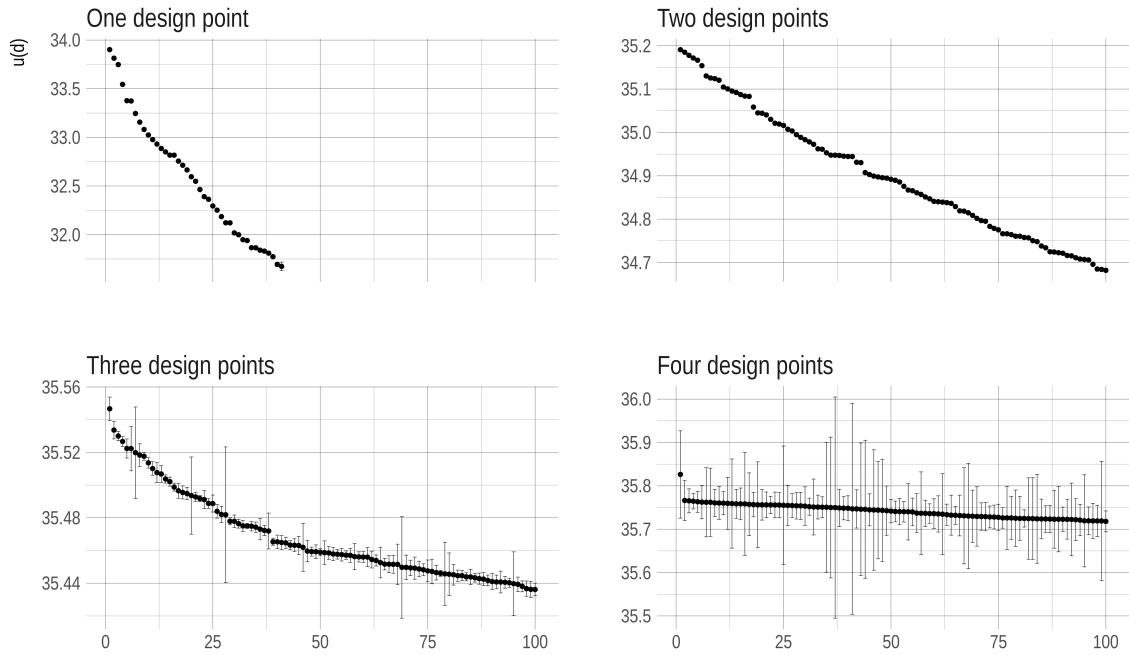


Figure 5: Estimated expected utilities (and central 95% intervals) for the top 100 designs with 1, 2, 3 and 4 timepoints.

There is much more uncertainty in expected utility estimates for the four design point problem and clearly many more simulations will be needed to pick out the optimal design. All that said, the differences in expected utility for all top 100 designs (of a given size) are quite small.

One advantage of our new algorithm (over Müller and Amzal) is that it is trivial to extend a search for an optimal design so long as the particle weights are retained from the previous run. A further advantage is that any extension to the optimal search run is not restricted to being on the same computer resource (desktop, cluster, cloud) as the initial run. This can be advantageous when determining the optimal design for a complex model which has a time consuming utility calculation as decisions on numbers of particles and their location can be amended easily (by the user) at each step of the algorithm. Also inspection of the (estimated) expected utilities can be examined at each step of the algorithm to determine how many steps are needed before the location of the optimal design is clear. For example, Figure 6 shows the top 100 three timepoint designs for steps $m = 0, 1, 2, 3$ and clearly shows that uncertainty around the top designs is sufficiently small that there is no need to extend the algorithm to step $m = 4$ to determine the top five designs in contention for being optimal design.

3.3 PK model

Ryan et al. (2015) focus on optimal design in a pharmacokinetic model of extra-corporeal membrane oxygenation in sheep. They model the observed concentration of a drug at time t as

$$y_t = \begin{cases} \frac{D}{T_{inf}k_eV} (1 - e^{-k_e t}) (1 + \varepsilon_t), & t \leq T_{inf} \\ \frac{D}{T_{inf}k_eV} (1 - e^{-k_e T_{inf}}) e^{-k_e(t-T_{inf})} (1 + \varepsilon_t), & t > T_{inf}, \end{cases}$$

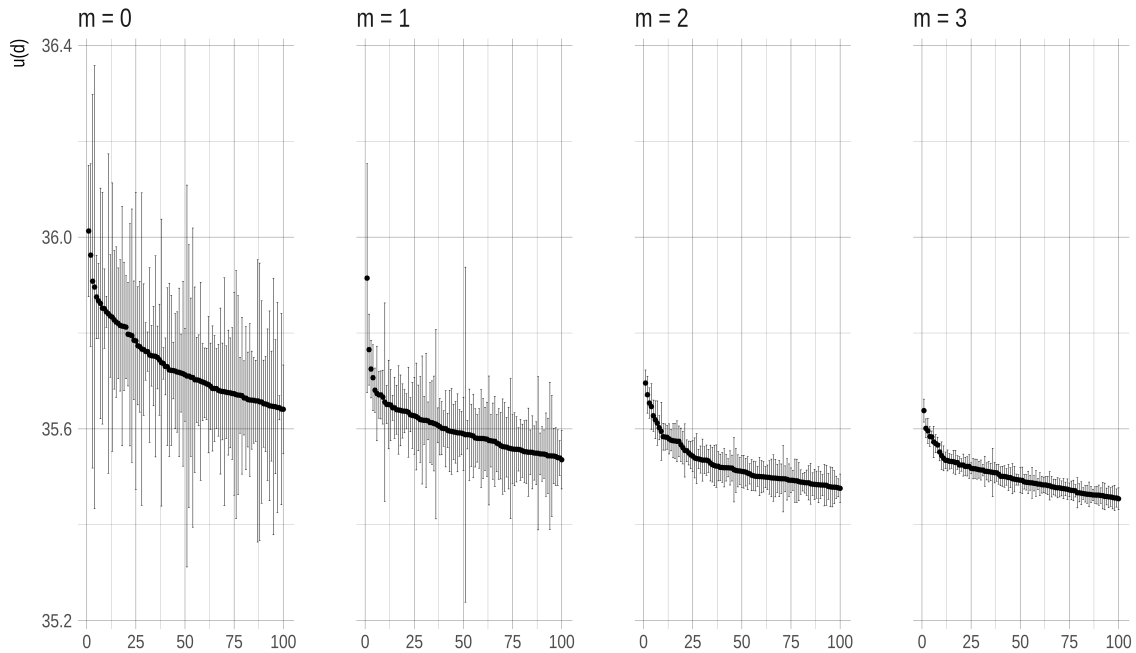


Figure 6: Estimated expected utilities (with central 95% confidence intervals) for the top 100 three timepoint designs for the aphid model using increasing values of m , with $\alpha_m = 2^{-m}$.

where $\varepsilon_t \stackrel{indep}{\sim} N(0, \sigma^2)$ and $t \in [0, T = 720]$ minutes. In their analysis, the dose level $D = 500 \text{ mg}$ is administered over a period of $T_{inf} = 30$ minutes. The two remaining (unknown) parameters are the volume of distribution V and the first-order elimination rate constant k_e .

Ryan et al. (2015) looks at one set of designs which replicate the same dosage profile and selects timepoints which optimise the precision of the peak concentration. This peak is proportional to $\phi = (1 - e^{-30k_e}) / (k_e V)$, and so the utility function here is $u(\mathbf{d}, \mathbf{y}) = 1 / \text{Var}(\phi | \mathbf{y})$. Prior uncertainty is expressed using independent components $\sigma^2 \sim \text{Ga}(10, 1000)$ and

$$\begin{pmatrix} k_e \\ V \end{pmatrix} \sim \text{LN}_2 \left\{ \begin{pmatrix} -3.26 \\ 8.99 \end{pmatrix}, \begin{pmatrix} 0.0071 & -0.0057 \\ -0.0057 & 0.0080 \end{pmatrix} \right\}.$$

Figure 7 shows the exact concentration and 100 stochastic simulations from the prior predictive distribution. A key feature is that the concentration increases until $t = 30$ (the value of T_{inf}) before decreasing. The plot also gives the optimal design determined by Ryan et al. (2015).

We found that $\text{Var}(\phi | \mathbf{y})$ could be estimated efficiently by running an MCMC algorithm with a simple independence proposal which proposes σ^2 from its prior and $(k_e, V)^T$ from a more diffuse version of its prior, in which its (co)variances on the log-scale are inflated to be 2.5 times larger. For each run of the MCMC algorithm we initialised the parameter values to those used to simulate the responses \mathbf{y} and found that very little burn-in was necessary. The number of iterations used in the MCMC algorithm was determined in an on-line manner: the effective sample size (ESS) was calculated every 5K iterations and further blocks of 5K iterations employed until the ESS exceeded 1K or a maximum of 500K iterations was achieved. For design points around the optimal, we typically only required between 5K and 20K iterations.

As in Ryan et al. (2015), we focus on searching for an optimal design which measures the process at time $t = 0$ and at $k = 10$ further time-points by using a Beta(a, b) design in which the time-points

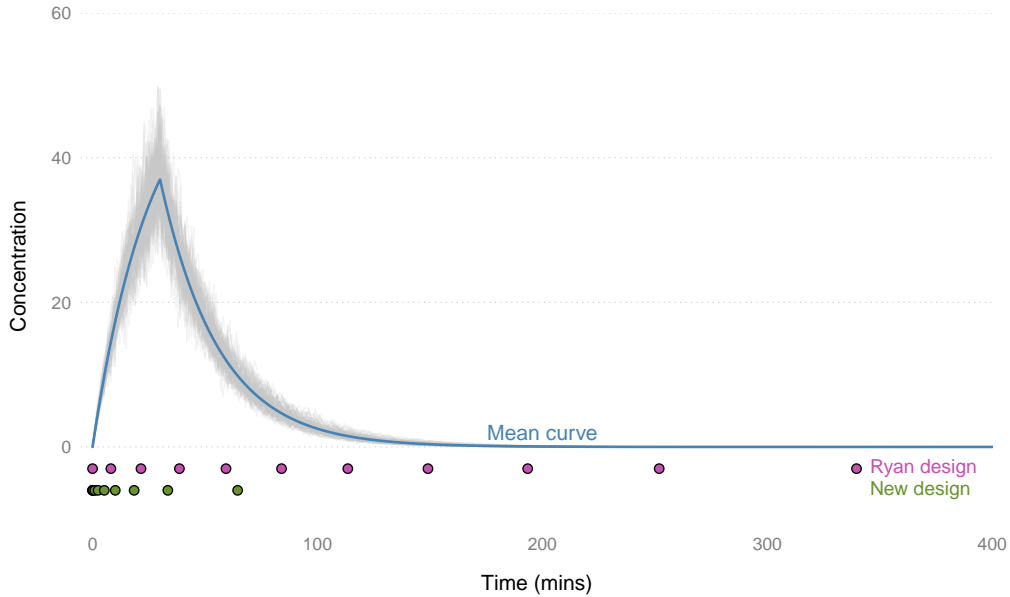


Figure 7: 100 simulations from the prior predictive distribution, together with the optimal design from Ryan et al. (2015) and that determined using the new algorithm.

are percentiles of the $\text{Beta}(a, b)$ distribution scaled to cover the full observation period $(0, T = 720]$. Thus the optimal design here is determined by appropriate choice of the parameters a and b . Ryan et al. (2015) used the Müller algorithm (with $J = 5$) to obtain an estimated optimal design using a computational budget of 24K utility evaluations. Figure 8a shows contours of the fifth power of (estimated) expected utility obtained using our algorithm with 24K utility evaluations. Note that this computation takes around six days on a typical single core machine, but only a single day on a six core machine. Clearly further computation will be needed to determine the optimal design but it is clear that its location is no where near that reported by Ryan et al. (2015). Figure 8b shows the designs visited during the run of the new algorithm and that it spent little time in the region of the Ryan et al. (2015) optimal design due to its relatively low expected utility.

Figure 8c shows the (estimated) expected utility for the top 100 designs, determined from a run of the new algorithm. Clearly there is too much uncertainty in the top designs to locate the optimal design. Note that, for comparison purposes, the expected utility for the Ryan et al. (2015) optimal design is around 0.6. To focus further on the optimal design we rented five 32 core machines in the Amazon cloud, each for six hours (spot instances), costing around US\$15. This resource delivered a further 30K utility evaluations and gave an updated list of the top 100 designs; see Figure 8d. The optimal design looks to be clear but perhaps would need confirming by doing further runs at the near-optimal design with a large uncertainty on its expected utility.

3.4 Conclusion

The search for Bayes optimal designs is time consuming as it requires the evaluation of the parameter posterior distribution (usually via MCMC) at very many datasets simulated from the prior predictive distribution. The search is further complicated because, in general, the expected utility function is fairly flat. Other methods target the optimal design by optimising a powered expected utility function. Instead we use a stepwise approach to focus in on designs in the upper tail of the distribution of expected utility, as this measure is much more intuitive.

The new algorithm presented in this paper is much more efficient in determining the optimal design in stochastic process models than others available in the literature. The particle representation

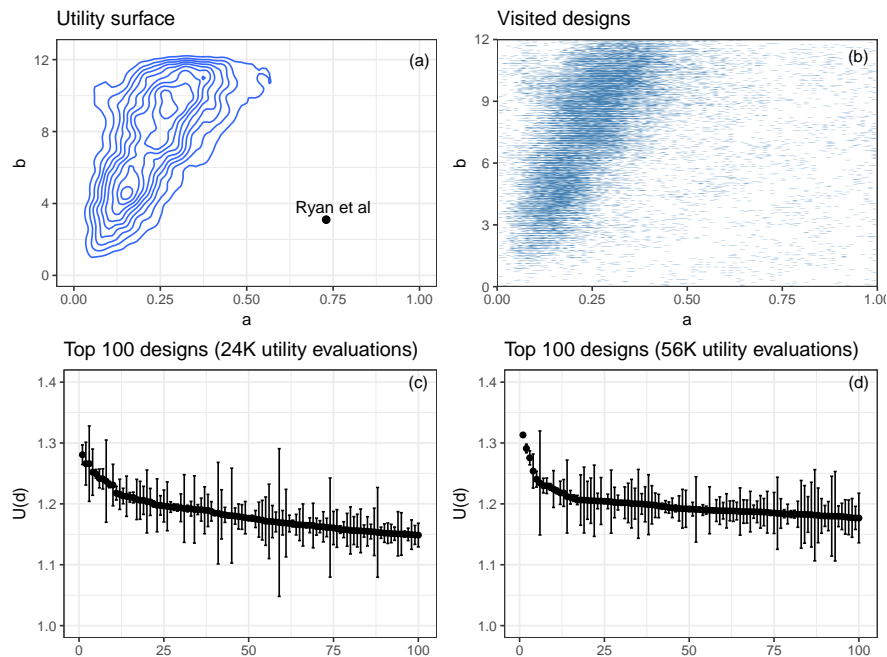


Figure 8: (a) Contours of $u(\mathbf{d})^5$ with (estimated) expected utilities obtained from the new algorithm using 24K utility evaluations. (b) Designs points visited during the run of the new algorithm. (c) Top 100 designs after 24K utility evaluations. (d) Top 100 designs after 58K utility evaluations.

over design space allows the algorithm to focus increasingly on regions of high utility. There are no issues of convergence in the scheme (as there are in, for example, the Müller scheme) and the output allows a simple comparison of (estimated) expected utility allowing for uncertainty in the estimates. The scheme is embarrassingly parallel and ideally suited to running on the cloud. The search for the optimal design is easily interrupted and restarted, allowing for the search to be monitored and additional compute resource to be added.

References

- Amzal, B., F. Y. Bois, E. Parent, and C. P. Robert (2006). Bayesian-optimal design via interacting particle systems. *Journal of American Statistical Association* 101, 773–785.
- Cook, A. R., G. J. Gibson, and C. A. Gilligan (2008). Optimal observation times in experimental epidemic processes. *Biometrics* 64(3), 860–868.
- Drovandi, C. C. and A. N. Pettitt (2013). Bayesian experimental design for models with intractable likelihoods. *Biometrics* 69(4), 937–948.
- Galassi, M., J. Davies, J. Theiler, B. Gough, G. Jungman, P. Alken, M. Booth, and F. Rossi (1996). Gnu scientific library.
- Gillespie, C. S. and A. Golightly (2010). Bayesian inference for generalized stochastic population growth models with application to aphids. *Journal of Royal Statistical Society, Series C* 59(2), 341–357.
- Henderson, D. A., R. J. Boys, K. J. Krishnan, C. Lawless, and D. J. Wilkinson (2009). Bayesian emulation and calibration of a stochastic computer model of mitochondrial DNA deletions in substantia nigra neurons. *Journal of the American Statistical Association* 104(485), 76–87.

- Khatab, A., E. H. Aghezzaf, C. Diallo, and I. Djelloul (2017). Selective maintenance optimisation for series-parallel systems alternating missions and scheduled breaks with stochastic durations. *International Journal of Production Research* 55(10), 3008–3024.
- Matis, J. H., T. R. Kiffe, T. I. Matis, and D. E. Stevenson (2007). Stochastic modeling of aphid population growth with nonlinear, power-law dynamics. *Mathematical Biosciences* 208(2), 469–494.
- Matis, T. I., M. N. Parajulee, J. H. Matis, and R. B. Shrestha (2008). A mechanistic model based analysis of cotton aphid population dynamics data. *Agricultural and Forest Entomology* 10(4), 355–362.
- Müller, P. (1999). Simulation-based optimal design. In *Bayesian Statistics 6: Proceedings of Sixth Valencia International Meeting*, Volume 6, pp. 459. Oxford University Press.
- Overstall, A. M. and D. C. Woods (2017). Bayesian design of experiments using approximate coordinate exchange. *Technometrics* 59(4), 458–470.
- Overstall, A. M., D. C. Woods, and M. Adamou (2017). *acebayes: Optimal Bayesian experimental design using the ACE algorithm*. R package version 1.4.1.
- Ryan, E. G., C. C. Drovandi, and A. N. Pettitt (2015). Fully Bayesian experimental design for pharmacokinetic studies. *Entropy* 17(3), 1063–1089.